ISSN 0303-402X, Volume 288, Number 4

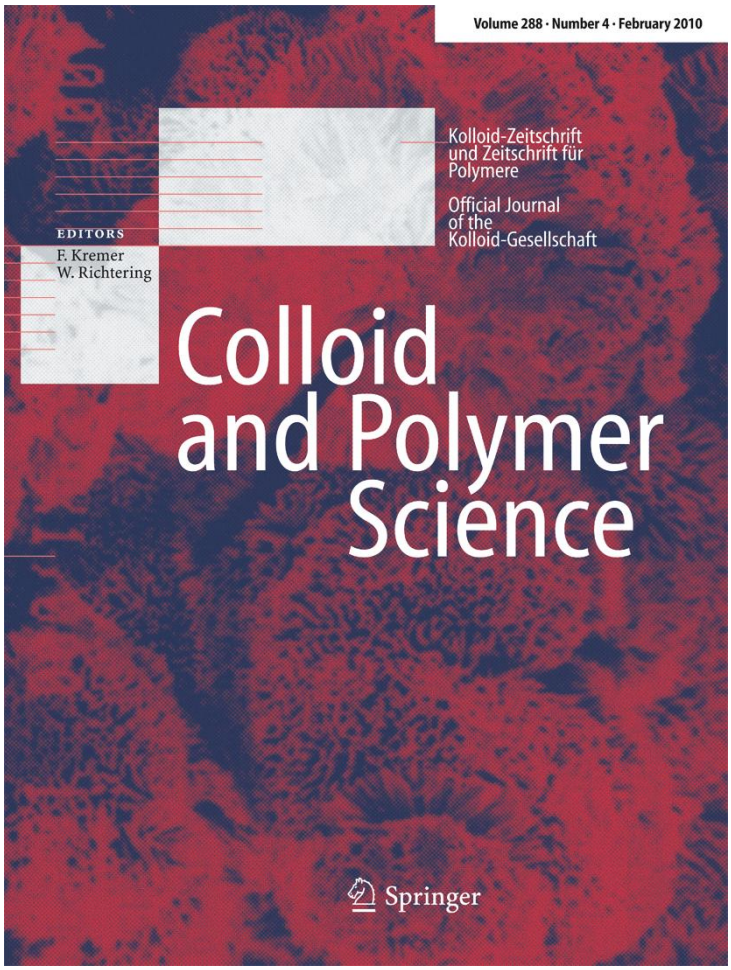

Colloid Polym Sci (2010) 288:449–459
DOI 10.1007/s00396-009-2170-5

ORIGINAL CONTRIBUTION

Ca^{2+}- and Mg^{2+}-induced molecular interactions in a dehydrocholic acid/didodecyldimethylammonium bromide mixed monolayer

Paula V. Messina · Juan Manuel Ruso · Gerardo Prieto · Marcos D. Fernández-Leyes · Pablo C. Schulz · Félix Sarmiento

Received: 21 October 2009 / Revised: 24 November 2009 / Accepted: 25 November 2009 / Published online: 7 January 2010

Abstract The aim of this article is the evaluation of Ca^{2+} and Mg^{2+} subphases presence effect on mixed monolayers composed by dehydrocholic acid (HDHC) and didodecyldimethylammonium bromide (DDAB). The monolayer stability was analyzed by the evaluation of thermodynamic parameters, ΔG_{mix}^{E} and α. At all calcium ion-tested concentration, the mixed systems X_{HDHC}=0.6 and 0.8 at π=30 mJ m^{-2} were always the most favored proportions. The X_{HDHC}=0.6 system was also stable in magnesium presence, and the X_{HDHC}=0.2-mixed monolayer went through a stable to an unstable state as the content of Ca^{2+} or Mg^{2+} augment. Finally, the X_{HDHC}=0.4 monolayer showed a particular behavior, i.e., remained stable at low cation concentration, unstable at intermediate concentration and stable again at high concentration. The effect was similar at Mg^{2+} presence.

Keywords Bile salts · Air-solution interface · Langmuir monolayers · Divalent cations · Monolayer stability

P. V. Messina (✉) · M. D. Fernández-Leyes · P. C. Schulz
Departamento de Química,
Universidad Nacional del Sur. CONICET-INQUISUR,
8000 Bahía Blanca, Argentina
e-mail: pau423ve@yahoo.com.ar

J. M. Ruso
Soft Matter and Molecular Biophysics Group,
Departamento de Física Aplicada, Facultade de Física,
Universidad de Santiago de Compostela,
15782 Santiago de Compostela, España

G. Prieto · F. Sarmiento
Biophysics and Interfaces Group,
Departamento de Física Aplicada, Facultade de Física,
Universidad de Santiago de Compostela,
15782 Santiago de Compostela, España

Introduction

Bile acids are steroidal amphipathic molecules derived from the catabolism of cholesterol. They modulate bile flow and lipid secretion, are essential for the absorption of dietary fats and vitamins, and have been implicated in the regulation of all the key enzymes involved in cholesterol homeostasis. Bile acids recirculated through the liver, bile ducts, small intestine, and portal vein to form an enterohepatic circuit. Their detergent properties aid in the solubilization of cholesterol in bile and of dietary fats and cholesterol in intestinal fluid, a prerequisite for their intestinal adsorption [1]. The high specificity and capacity of bile acid transport system during enterohepatic circulation might form the basis of current research on drug-bile acid systems for specific drug targeting and for improving the intestinal absorption of poorly adsorbed and non-adsorbed drugs, such as peptides [2].

After entering inside the amphiphiles aggregates, bile acid type molecules lie flat at the aggregate surface between head groups of the conventional amphiphiles. In turn, the large steroid skeleton forces these head groups apart from each other [3–5]. Hence the addition of a bile acid to the amphiphile aggregates usually increases the average head group areas (referred to as the steric effect of a bile acid) and transform these aggregates into highly curved ones (i.e., a bile acid-induced vesicle to micelle transitions) [6–10].

In a previous work [11], we evaluated the effect of a bile acid-type molecule (dehydrocholic acid (HDHC)) intercalation in the structure of a monolayer composed by a cationic surfactant (didodecyldimethylammonium bromide (DDAB)). The effects of steric and electrostatic interactions between both components were evaluated through the use

of a constant surface pressure penetration Langmuir balance based on Axisymmetric Drop Shape Analysis (ADSA). The experiments were performed as a previous step to the use of the tested surfactants as structural units for construction of more complex supramolecular assemblies.

As a continuation of that study, this article examines the effect of divalent cations on HDHC/DDAB monolayers. The interactions of both components on a mixed monolayer are modulated extrinsically by mobile ions in the surrounding medium [12, 13]. Divalent alkali cations such as Ca^{2+} and Mg^{2+}, in particular, bind and provide positive charges on surfaces [14]. Consequently, electrostatic repulsion causes membrane separation [15, 16]. We paid a special attention to understanding the effect of each composition on system stability which may be useful in getting better formulation of the final products. Parameters such as temperature, surface pressure, molecular area, compressibility, number of coexisting phases, were directly and simultaneously measured and evaluated. The thermodynamics of mixing was also analyzed.

The information gathered here may be useful to complete the knowledge of the complex aggregation behavior of bile acids and related compounds, which are very important for the understanding of their interaction with biological membranes, billiary secretions, or cholesterol solubilization. HDHC is a scarcely studied bile salt derivative, which adds interest to this work.

Experimental methods

Materials

HDHC was from Dr. Theodor Schuchardt (Munich) and DDAB was obtained from Sigma. Both compounds were of analytical grade (99% pure) and were used as purchased. Calcium nitrate ($Ca(NO_3)_2$, Sigma 99%) and magnesium nitrate ($Mg(NO_3)_2$, Sigma 98%) were dissolved in Milli-Q water (pH=6.0) using a magnetic stirrer to obtain an ion subphase concentration of 10, 20, and 40 mM.

Apparatus and operation conditions

The experiments were performed with a constant surface pressure penetration Langmuir balance based on ADSA [17–19]. The whole setup, including the image capturing, the micro-injector, the ADSA algorithm, and the fuzzy pressure control, is managed by a Windows integrated program. A solution droplet is formed at the tip of a capillary, which is outer one of an arrangement of two coaxial capillaries connected to the different branches of a micro-injector. These can operate independently, permitting one to vary the interfacial area by changing the drop volume, and to exchange the drop content by through flow. The software first detects the drop and with an appropriate calibration, transforms it into physical coordinates. Then the experimental drop profiles, extracted from digital drops micrographs, are fitted to the Young-Laplace equation of capillarity by using ADSA. This process is performed automatically, the liquid density difference and the local gravity being the only inputs and yielding as outputs the drop volume V, the interfacial tension γ, and the surface area A in about 0.3–5 s for each picture, depending on the required precision. Area control uses a modulated fuzzy logic proportional, integral, and derivative control algorithm and is controlled by changing the drop volume. During the experiment, the drop is immersed in a thermostated and vapor-saturated standard spectrophotometer cuvette (Hellma®) minimizing contamination and drop evaporation. The surface pressure is obtained from the relationship $\pi=\gamma_0-\gamma$, where π is the surface pressure; γ and γ_0 are the surface tension of the subphase liquid covered with and without the monolayer. The setup is placed on a pneumatic vibration-damped optical bench table in a clean laboratory. All experiments were performed at (25.0±0.1)°C. Temperature was maintained by a thermostat bath with recycling water throughout all the experiment. The curves were highly reproducible: each experiment was done three times, the standard deviation [19] on π and A was estimated to be ±0.01 mJ m^{-2} and ±0.005 nm^2 mol^{-1}, respectively. Equation fitting were done from non-linear procedures using ORIGIN® computer package (release 7.0).

Monolayers

Spreading solutions of HDHC and DDAB and their mixtures were prepared dissolved in a methanol/chloroform mixture (1:4) to obtain solutions of (7×10^{-5} M) total concentration. Then an aliquot of 1.2 μL was spread on the surface using a micro-syringe. Once the spreading solvent has evaporated (4 min were allowed) and consequently the amphoteric molecules were confined to a monomolecular film at the subphase-air interface, the program started the expansion until a volume of 25 μL at a rate of 0.2 μL s^{-1}. When expansion was finished, the drop area was maintained constant for 118 s (the time required for the studied monolayers to reach the thermodynamic equilibrium) and then the compression started at the same rate of the expansion process.

Theoretical methods

In order to analyze the response of the adsorbed molecules to interface compression [20–24], the area

modulus (C_s^{-1}) has been estimated from the equilibrium relationship between interfacial pressure (π) and interfacial area (A):

$$C_s^{-1} = -A\frac{d\pi}{dA} \quad (1)$$

We examined the influence of electrostatic, hydrophobic and hydration forces contributions, analyzing their effect on the limiting molecular area values (which correspond to the maximum monolayer compression). An ideal mixed monolayer and a completely immiscible monolayer are absolute opposite. However, both follow Eq. 2. In an ideal mixed monolayer of components 1 and 2, the intermolecular force $F_{11}=F_{12}=F_{22}$ whereas in a completely immiscible monolayer $F_{11}>>F_{12}<<F_{22}$, where F_{12} represents the attractive forces between molecules of the two dissimilar components.

The limited area per molecule for an ideal two-component mixed monolayer, $(A_{1,2})_{\pi,\text{ideal}}$, can be calculated from:

$$(A_{1,2})_{\pi,\text{ideal}} = X_1(A_1)_\pi + X_2(A_2)_\pi \quad (2)$$

where X_1 and X_2 are the mole fractions of the components 1 (DDAB) and 2 (HDHC) at the mixed spread monolayer, $(A_1)_\pi$ and $(A_2)_\pi$ are the molecular area of the pure monolayers of components 1 (HDHC) and 2 (DDAB) at an identical surface pressure (π). The excess area, $(A_{ex})_\pi$, for a binary monolayer can be expressed as:

$$(A_{ex})_\pi = (A_{1,2})_{\pi,\text{exp}} - (A_{1,2})_{\pi,\text{ideal}} \quad (3)$$

where $(A_{1,2})_{\pi,\text{exp}}$ is the collapse area per molecule of the mixed monolayer. $(A_{1,2})_{\pi,\text{exp}}$; $(A_1)_\pi$ and $(A_2)_\pi$ can be obtained from the corresponding π-A isotherms and were taken as the point where the upper part of the curve starts to deviate from the straight line [25]. According to the two-dimensional phase rule, if two surfactants are miscible in Langmuir monolayers only one limiting pressure value is observed. The isotherm of a monolayer consisting of two immiscible components will show distinct limiting pressure values corresponding to those of the two pure component monolayers, which are independent of the additive monolayer composition. The excess area of an ideally mixed monolayer or a one formed by two components completely immiscible will be zero and a plot of $(A_{1,2})_{exp}$ vs. X_1 at a given surface pressure will be a straight line. Any deviation from the straight line merely indicates miscibility and non-ideality of mixing.

The net interaction between two components in a mixed monolayer, at a constant surface pressure π and absolute temperature T, can be evaluated from the calculation of excess Gibbs energy $(\Delta G_{mix}{}^E)$, the Gibbs energy of mixing (ΔG_{mix}), and the interaction parameter (α) [20, 23, 26], which are given by:

$$\Delta G_{mix}{}^E = \int_0^\pi [A_{1.2} - (X_1A_1 + X_2A_2)]\, d\pi \quad (4)$$

$$\alpha = \frac{\Delta G_{mix}^E}{RT\left(X_1X_2^2 + X_2X_1^2\right)} \quad (5)$$

and

$$\Delta G_{mix} = \Delta G_{mix}^{id} + \Delta G_{mix}^E \quad (6)$$

where the first term, the ideal Gibbs energy of mixing (ΔG_{mix}^{id}), can be calculated from the equation:

$$\Delta G_{mix}^{id} = RT\,(X_1 \ln X_1 + X_2 \ln X_2) \quad (7)$$

R is the universal gas constant.

Results and discussion

Cations effect on monolayer structure

The area modulus C_s^{-1} is a valuable tool which can be used to classify the monolayer physical state. It provides information about the layer structures; high elasticity values are associated with a film that has strong cohesive interfacial structure. A maximum in the C_s^{-1} vs. A plot is related to a configurational transition in the monolayer structure [27]. Actually the C_s^{-1} vs. A curve is another form to evaluate the change of surface pressure during compression and will be better to expose the monolayer state. Values of C_s^{-1} ranging from 0 to 12 mJ m^{-2} are characteristic of the gaseous state of a monolayer; values ranging from 12 to 100 mJ m^{-2} correspond to the liquid-expanded state, from 100 to 250 mJ m^{-2} are characteristic of liquid-condensed state, and above 250 mJ m^{-2} indicate the solid state of a film. As an example of the computed data Figs. 1, 2, and 3 show the variation of surface pressure and C_s^{-1} vs. molecular area (A) for the $X_{HDHC}=0.8$ mixed system spreaded on water subphase, on 20 mM Ca^{2+} and 20 mM Mg^{2+} solutions, respectively. The mixed system composed by $X_{HDHC}=0.8$ spreaded on water subphase (Fig. 1) presented a LE monolayer until $A=0.84$ nm^2mol^{-1} followed by a LE–LC phase coexistence region (plateau region in the π vs. A plot) and finally a LC phase ($A=0.65$ nm^2 mol^{-1}). The liquid condensed phase existed until an area of 0.61 nm^2 mol^{-1} were a new phase transition occurred. The monolayer did not show a visible transition to the solid state (S), the second change that was observed could be associated to a rearrangement of molecules in the

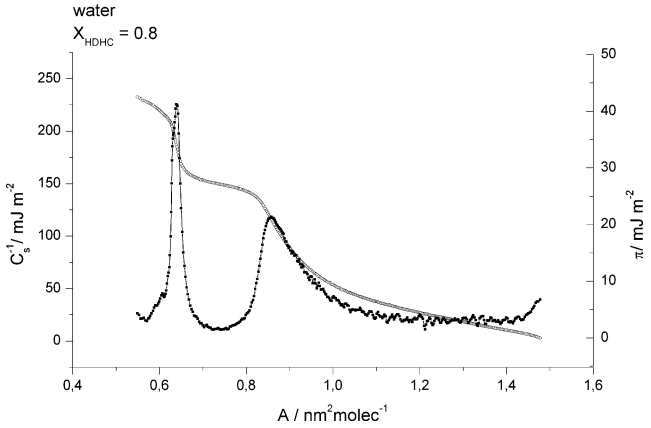

Fig. 1 π vs. A and C_s^{-1} vs. A plots for X_{HDHC}=0.8 mixed system spreaded on water subphase

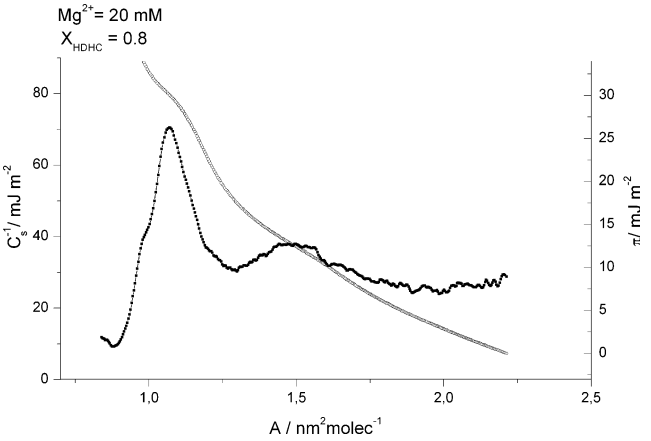

Fig. 3 π vs. A and C_s^{-1} vs. A plots for X_{HDHC}=0.8 mixed system spreaded on 20 mM Mg^{2+} water solution subphase

LC phase. The area modulus (C_s^{-1}) increased distinctively till nearly 250 mJ m^{-2}, showing a highly condensed monolayer. For such system, the C_s^{-1} vs. A plot showed two maximum peaks at 0.85 and 0.62 nm^2mol^{-1}, respectively, attributed to the LE→LC and LC→-LC′ transitions. A similar behavior was seen when the same system was spreaded on a 20 mM Ca^{2+} solution, Fig. 2. However, the cation presence eliminated the phase coexistence region. Two maximum peaks at the C_s^{-1} vs. A plot (corresponding to the LE→LC and LC→LC′ transitions) appeared at superior molecular areas values (1.20 and 1.12 nm^2mol^{-1}, respectively). When Mg^{2+} was present instead Ca^{2+} a less condensed monolayer was appreciated (low C_s^{-1} and high A values). The C_s^{-1} vs. A plot showed only one maximum. It is related to the LE→LC transition.

From analysis of π vs. A and C_s^{-1} vs. A plots for all HDHC/DDAB mixtures the corresponding phase diagrams were constructed. The obtained results were shown in Figs. 4 and 5.

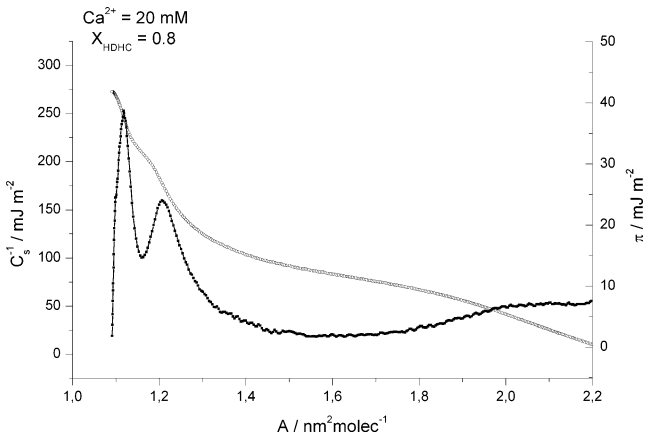

Fig. 2 π vs. A and C_s^{-1} vs. A plots for X_{HDHC}=0.8 mixed system spreaded on 20 mM Ca^{2+} water solution subphase

Water subphase

Figure 4a shows the phase diagram of pure and mixed systems spreaded on water subphase. For the mixed X_{HDHC}=0 to 0.6 monolayers, the phase sequence on compression was gas + LE→LE→LE-LC→LC. When $0.6<X_{HDHC}<1$, the increment of π (over π=35 mJm^{-2}) caused a transition to the LC′ phase. In a previous work, we determined that the behavior of such amphiphiles in the monolayer was clearly non-ideal and would be seriously influenced by the amount of HDHC molecules present. The presence of bile acid type molecules caused that the monolayer was more condensed and that the intermolecular attractive interactions were stronger. This fact would be related to H-bond formation between water and carboxilate and carbonile groups in the cholesteric ring and agreed with the existence of laterally structured microdomains at the monolayer [11].

Ca^{2+}

For the systems spreaded on [Ca^{2+}]=10 mM aqueous solution, Fig. 4b, the phase sequence was: gas + LE→LE→LE + LC→LC. The presence of Ca^{2+} ion eliminated the LC-LC′ interfacial phase coexistence. The same effect probably has caused the vanishing of the LE-LC phase coexistence region as the proportion of bile acid at the monolayer augmented (X_{HDHC}>0.8) at [Ca^{2+}]= 20 mM, Fig. 4c.

At a [Ca^{2+}]=40 mM subphase concentration, an important expansion of the molecular area was appreciated, Fig. 4d. The zone of molecular areas for where there was a LE-LC phase coexistence region diminished with the increment of the amount of the bile acid at the mixed monolayer. For $X_{HDHC}\geq$0.8 systems, such region disappeared. This fact revealed a notably dependence of

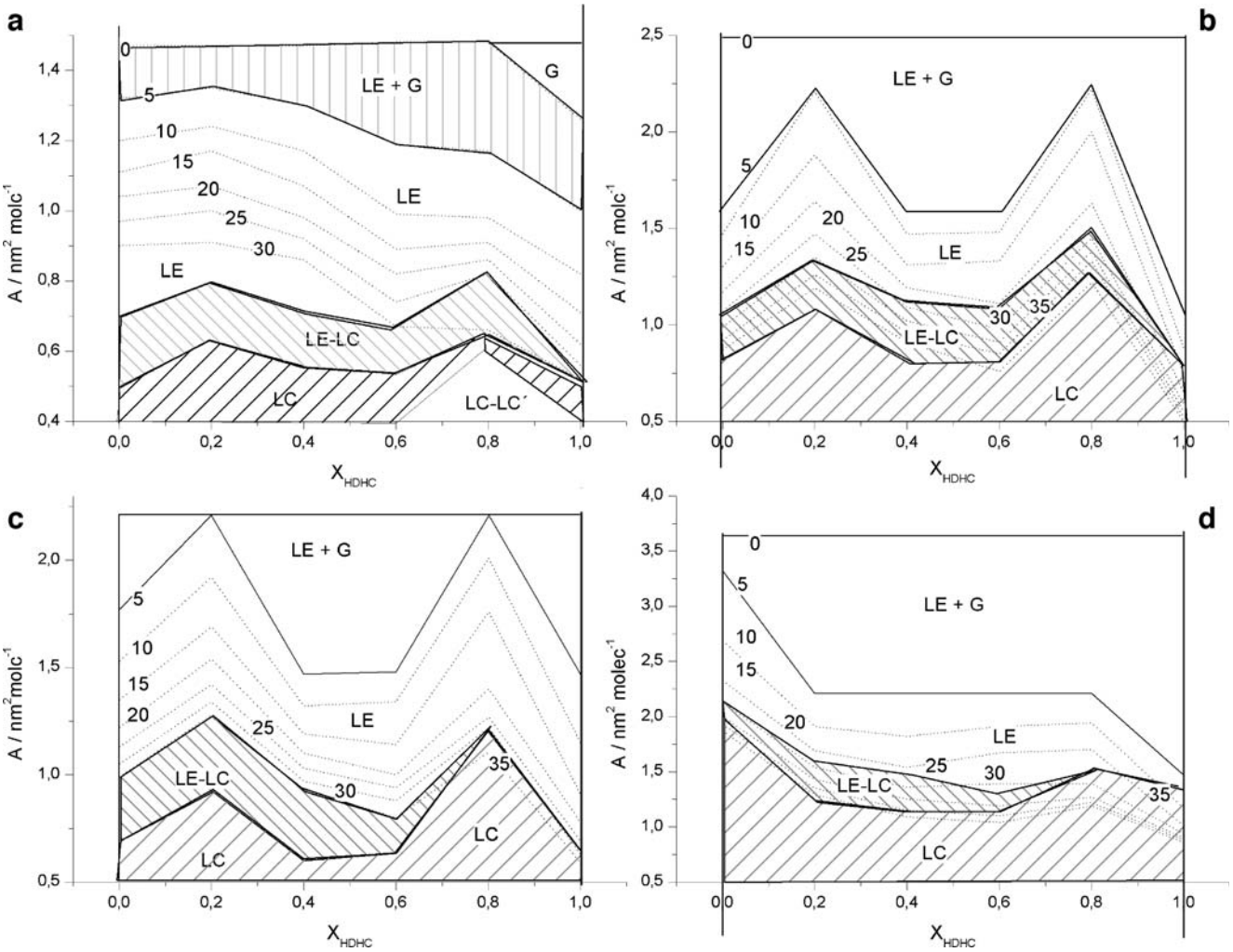

Fig. 4 Phase diagram of HDHC/DDAB mixed monolayers at different subphase Ca^{2+} concentrations: **a** $[Ca^{2+}]=0$; **b** $[Ca^{2+}]=10$ mM; **c** $[Ca^{2+}]=20$ mM; **d** $[Ca^{2+}]=40$ mM. *Dashed lines* correspond to surface pressure

monolayer behavior with the increment of the amount of HDHC molecules and Ca^{2+} ions at the interface.

For a deep analysis of such behavior, we evaluated the relationship that existed between the limiting and the excess area, computed by Eq. 3, with the monolayer compositions, Fig. 6. The ideal composition dependence of limited molecular area, calculated by Eq. 2, was also included. At low subphase Ca^{2+}content, limiting molecular area of pure DDAB was the usual for dialkyldimethylammonium bromide monolayers $\left(\left(A_{1,2}\right)_{\pi}^{\mathrm{DDAB}}, = 0.78\ \mathrm{nm^2 mol^{-1}}\right)$ [28–30]. Comparing the obtained results with the molecular cross-sectional area (c.a. 0.40 $\mathrm{nm^2 mol^{-1}}$[31]) of the close-packed double chain quaternary ammonium salts, we assumed that DDAB molecules took a conformation with both alkyl chains lying with a certain angle at the surface. For the pure HDHC monolayer, $\left(A_{1,2}\right)_{\pi,}^{\mathrm{HDHC}} = 0.46\ \mathrm{nm^2 mol^{-1}}$ was similar to that of cholanoic acid [32]. We inferred that at low surface pressure the steroid nucleus of bile acid lied parallel to the aqueous interface but assumed a vertical position upon compression. Similar results were obtained for such systems spread on pure water subphase [11]. The increment of subphase ion content, $[Ca^{2+}]=20$ mM, caused an augment of both pure and mixed systems limited area values, showing an expanding effect. Such positive deviation would be assumed to strongly electrostatic forces between polar head groups. The presence of positive ions overcharge the slightly dissociated acid (the measured ionization degree of HDHC was about 0.1 [33]), so that the acid is converted to a pseudo –cationic surfactant. These behavior was superior for $X_{\mathrm{HDHC}}=0.2$ and 0.8 monolayers, that was for such system composed for high content of DDAB or HDHC. So the monolayer became less condensed.

A different situation could be observed when $[Ca^{2+}]=40$ mM. In such conditions $\left(A_{1,2}\right)_{\pi}$, values showed a significant negative deviation from ideality $\left(\left(A_{\mathrm{ex}}\right)_{\pi} < 0\right)$.

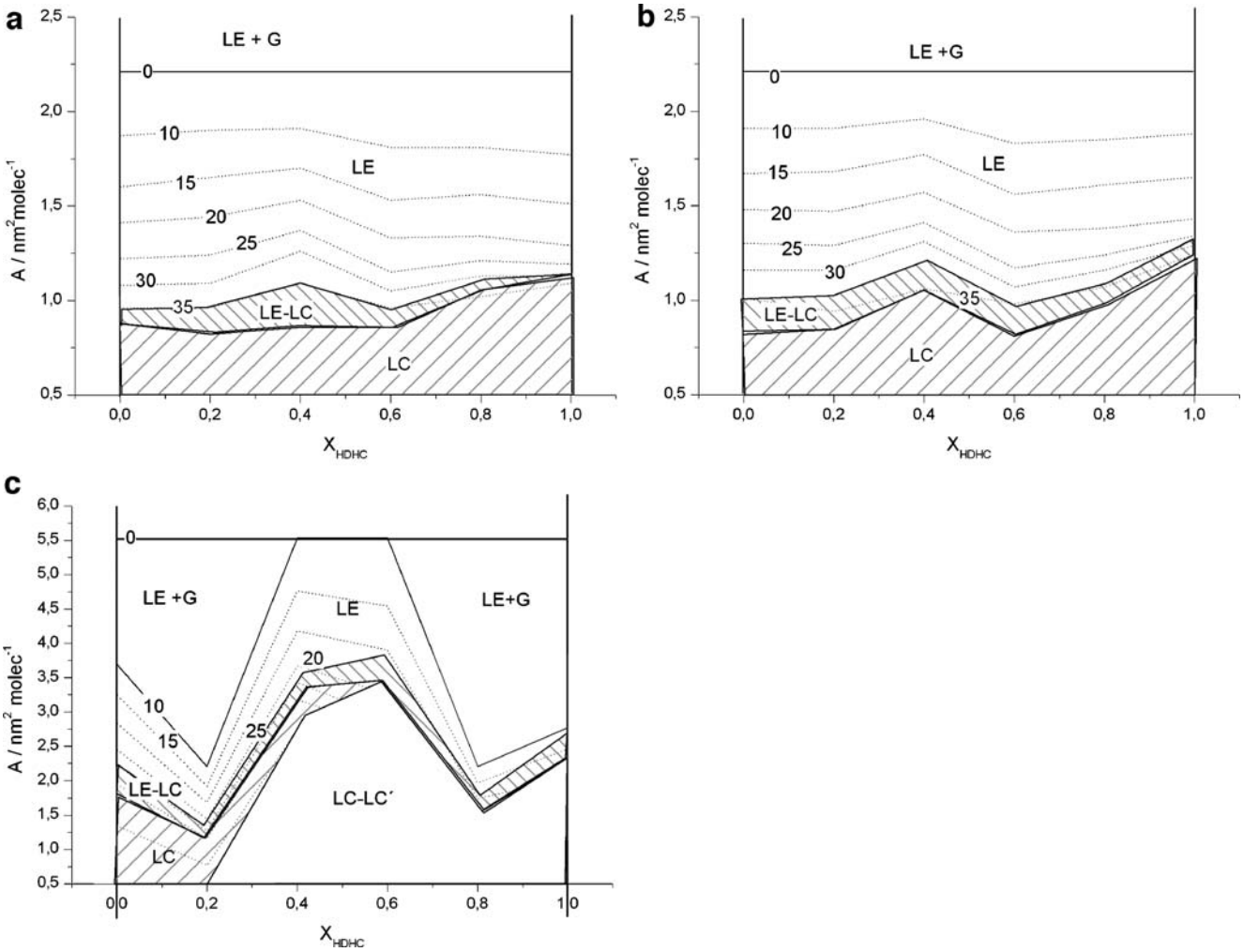

Fig. 5 Phase diagram of HDHC/DDAB mixed monolayers at different subphase Mg^{2+} concentrations: **a** [Mg^{2+}]=10 mM; **b** [Mg^{2+}]=20 mM; **c** [Mg^{2+}]=40 mM. *Dashed lines* correspond to surface pressure

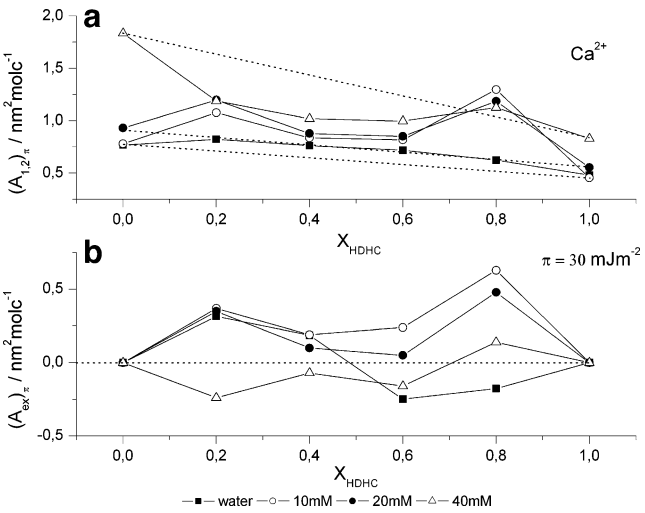

Fig. 6 **a** Limited area ($A_{1,2}$) and **b** excess area (A_{ex}), computed by Eq. 3)—monolayer composition (X_{HDHC}) dependence at different calcium ion concentrations. *Dashed lines* in **a** correspond to ideal molecular areas values $\left((A_{1,2})_{\pi,\text{ideal}}\right)$ computed by Eq. 2

The difference between the theoretical and experimental molecular areas in the condensed region can be explained by a loss of water molecules from the monolayer.

Many phenomena in colloid, polymer and interface science that involve electrolytes shown pronounced ion specificity. More than a century ago, Franz Hofmeister noted a particular ordering of ions in the ability of salts of a common counterion to precipitate egg-white proteins [34]. It was thought that an ion's influence on macromolecular properties was caused at least in part by "making" or "breaking" bulk water structure. The ions called kosmotropes, which were believed to be "water structure makers" are strongly hydrated and have stabilizing effects on proteins. On the other hand, ions called chaostropes were water structure breakers and are known to destabilize folded proteins [35]. For specific ions effects in solution or at more complex surfaces, only empirical rules are known. Recently, a simple "low of matching water affinities" has been proposed by Collins [36]. It relates the tendency of

oppositely charged ions to spontaneously associate as inner sphere ion pairs in aqueous solution to matching absolute free energies of ion hydration. This is supposed to be due to the fact that the strength of interaction between the ions and the water molecules is correlated to the strength with which the ions interact with each others. Following Collins's concept, chaotropes can form direct ions pairs with other chaotropes, much as kosmotropes with other kosmotropes, but chaotropes do not come into close contact with kosmotropes. Thus, it was concluded that oppositely charged ions in free solution spontaneously form inner sphere ion pairs only when they have equal water affinities.

Dehydrocholate ion (DHC^-) behaves as a water-structure breaker (chaostrope). The structure of hydrocarbon hydration cages is affected by the solubilized hydrocarbon size and shape, and some hydrocarbons which may not enter the hydrophobic hydration cages act as structure breakers. The large size and the stiffness of the steroid backbone and the presence of the polar groups in different part of the molecule hindered the formation of a structured water cage surrounding the surfactant molecule and favored the destruction of the "water icebergs". This increased the number of "free" (less-hydrogen-bonded) water molecules [37].

In agreement with Collins's concept the interaction of DHC^- (chaotrope) ion with Ca^{2+} (chaotrope) eliminated the H-bond formation between water and carboxilate and carbonile groups of bile acid molecule. Thus, this ion pair or dipole would be much less hydrated than separate ions and headgroups. This smaller hydration was reflected in reduction of effective headgroups areas resulting in a more condensed monolayer.

Mg^{2+}

Magnesium ion effect on the monolayer phase's behavior was seen in Fig. 5. All mixtures behaved largely as a liquid expanded system at low pressures. The gas phase did not come to be appreciated, which was due to the highly orientated coordination structures induced by magnesium. The LE-LC phase coexistence region ($\pi \geq 30$ mJ m^{-2}) was restricted to a small zone of molecular areas. Further compression provoked the appearance of LC phase. Higher ion concentration (40 mM) caused a different behavior, Fig. 5c, i.e., when $X_{HDHC} \leq 0.2$ and low π the systems existed in a gaseous + LE phase; a little augment of surface pressure favored LE phase and finally a LE→LC transition was seen. For $X_{HDHC} > 0.2$ systems, a molecular rearrange was seen at the LC phase. For the $0.4 \geq X_{HDHC} \leq 0.6$ systems, the gaseous phase disappeared showing a condensing effect and from $X_{HDHC} \geq 0.6$, gaseous phase was observed again at low surface pressures, but LC phase disappeared.

The analysis of $(A_{1,2})_\pi$, and A_{ex} vs. X_{HDHC} plots, Fig. 7, let us to corroborate that a highly molecular areas

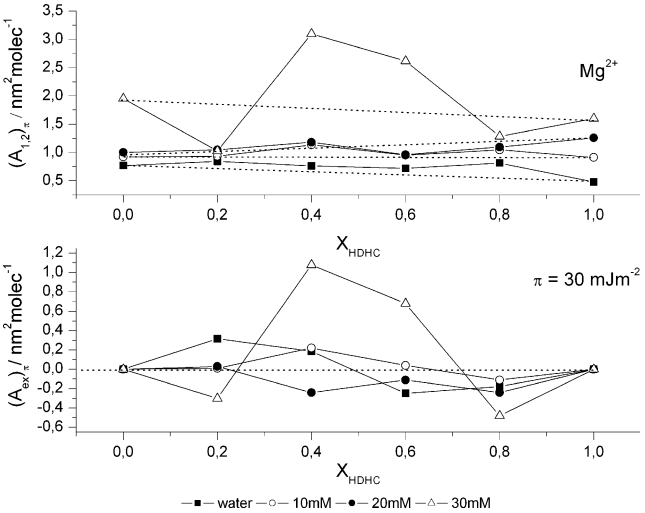

Fig. 7 **a** Limited area ($A_{1,2}$) and **b** excess area (A_{ex}), computed by Eq. 3)—monolayer composition (X_{HDHC}) dependence at different magnesium ion concentrations. *Dashed lines* in **a** correspond to ideal molecular areas values $\left((A_{1,2})_{\pi,\text{ideal}}\right)$ computed by Eq. 2

expansion effect was seen when Mg^{2+} ion was present at the subphase instead Ca^{2+}. For such conditions, the value of $(A_{1,2})_{\pi,}^{HDHC}$ was highly superior than the cross-sectional area of steroid group (≈0.40 $nm^2 mol^{-1}$) and than the bile acid molecular length (≈1.30 nm) [38]. These facts showed the existence of very poorly condensed monolayers. The value of $(A_{1,2})_{\pi,}^{DDAB}$ oscillated between 0.92 to 1.25 nm^2 mol^{-1} with the augment of Mg^{2+} subphase concentration.

In an analysis of the binding of metal ions to carboxyl groups, it was found that magnesium apparently always bind in a monodentate manner, show the strong propensity to assume an octahedral structure with all O–Mg–O angles near to 90°, and to bind strongly to water molecules. In carboxylated complexes, Mg^{2+} is likely to retain at least one water ligand in its first coordination shell [39]. Such behavior implied that the intercalation of the partially hydrated Mg^{2+}, between carbonile groups on bile acid molecules caused a major disruption of the monolayer than Ca^{2+} noticing an expanded effect.

Mixed monolayers presented negative deviations respect ideality, except for X_{HDHC} 0.4 at $[Mg^{2+}]$=10 mM; X_{HDHC} 0.4 and 0.6 at $[Mg^{2+}]$=40 mM. The presence of hydrated ion at the monolayer provoked both repulsive and steric interactions. To solve this problem we supposed that some bile acid molecules were expelled from the interface by compression. Water-insoluble HDHC became soluble in coordination with cations.

Cations effect on monolayer stability

The two components interactions and the thermodynamic stability of the mixed monolayer was investigated from the

evaluation of the excess free energy $\left(\Delta G_{\mathrm{mix}}{}^{\mathrm{E}}\right)$, the free energy of mixing (ΔG_{mix}), and the interaction parameter (α) computed by Eqs. 4–7.

The negative sing of $\left(\Delta G_{\mathrm{mix}}{}^{\mathrm{E}}\right)$ is considered as a criterion of monolayer stability, whereas a positive value can suggest phase separation in the monolayer. The interaction parameter is closely related to ΔG_{mix} and has a similar sense. The minimum values of α indicates the mixed monolayer composition at which the strongest interaction between both components occurs. The negative sign of α means that the interactions between unlike molecules in a binary 2D-mixture are more attractive than between like molecules, whereas a positive sign of this parameter indicates that the interactions between unlike molecules are repulsive or at least less attractive than between like ones in a one-component monolayer [40]. There is no sense in calculating such parameters for immiscible systems. It can be seen that the limited areas values of the mixed monolayers (Figs. 6 and 7), presented a close relationship with composition. Consequently, it could be concluded that all monolayers were miscible.

Plots of α vs. X_{HDHC} dependencies were shown in Fig. 8 and provided some additional information to that from the $\left(\Delta G_{\mathrm{mix}}{}^{\mathrm{E}}\right)$ values (Table 1). From the inspection of Table 1 and Fig. 8, it can be seen that almost all mixed compositions were stable at Ca^{2+} ion presence, this behavior augmented with compression. The best favored proportions were X_{HDHC}=0.2, 0.6, and 0.8. As the Ca^{2+} concentration augmented, electrostatic repulsion appeared. So, positive values of α appeared for the X_{HDHC}=0.4 monolayer at [Ca^{2+}]=20 mM. The X_{HDHC}=0.2, 0.6, and 0.8 systems continue to be stable with the increment [Ca^{2+}], but the interaction parameter diminished.

At 40 mM Ca^{2+} subphase concentration, it was observed that the X_{HDHC}=0.2 mixed system presented positive α values at all surface pressures, while X_{HDHC}=0.4, 0.6 and 0.8 were stable.

The X_{HDHC}=0.2 mixed monolayer (with high content of DDAB) presented an increment of α value with the augment of Ca^{2+} ion amount at the subphase. Such fact is probably due the existence of electrostatic repulsion between Ca^{2+} and $R_2N^+(CH_3)_2$ groups. At low ion content, the $-COO^-$ groups in bile acid steroidal backbone neutralized Ca^{2+} and stabilized the monolayer. Nevertheless as the Ca^{2+} concentration at the subphase augmented, the $-COO^-$ groups were not enough to disperse positive charges and repulsive interaction with DDAB groups occurred.

Similar behavior was appreciated for the rest of mixed systems but as the amount of bile acid molecules at the

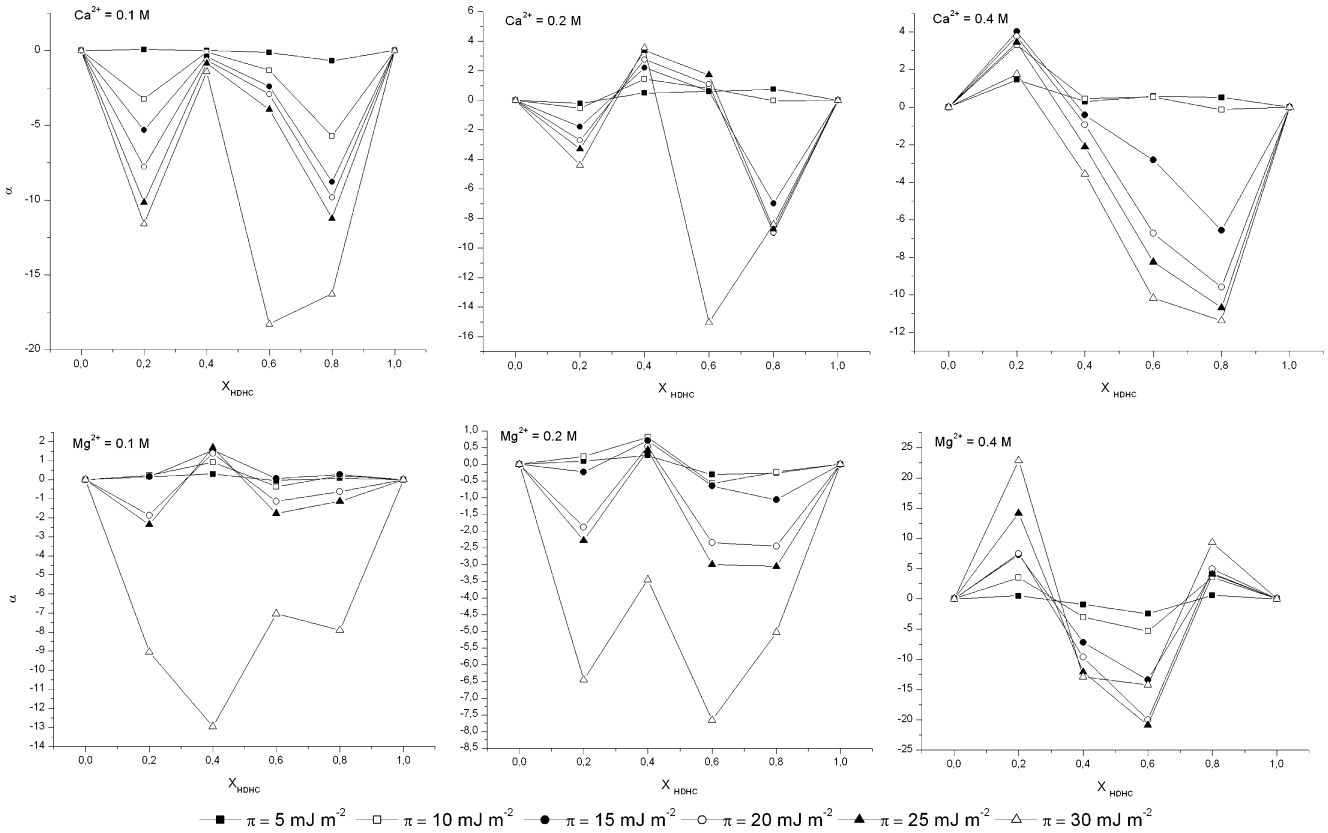

Fig. 8 Interaction parameter (α) vs. X_{HDHC} plots at different surface pressures and ion subphase concentration

Table 1 Variation of the excess free energy of mixing $(\Delta G_{mix}{}^{E})$ for the HDHC/DDAB systems on different calcium and magnesium subphase concentration

	$\Delta G_{mix}{}^{E}$/kJ m^{-2}			
π/mJ m^{-2}	X_{HDHC}=0.2	X_{HDHC}=0.4	X_{HDHC}=0.6	X_{HDHC}=0.8
[Ca^{2+}]=0.1 M				
5	−0.035±0.003	−0.012±0.003	−0.074±0.009	−0.261±0.073
10	−1.283±0.526	−0.051±0.026	−0.787±0.092	−2.263±0.323
15	−2.113±0.812	−0.231±0.056	−1.424±0.101	−3.485±0.492
20	−3.08±0.725	−0.374±0.012	−1.745±0.099	−3.897±0.384
25	−4.03±0.912	−0.5122±0.069	−2.345±0.123	−4.457±0.501
30	−4.59±0.689	−0.835±0.077	−10.88±2.569	−6.454±0.704
[Ca^{2+}]=0.2 M				
5	−0.082±0.013	−0.133±0.053	−0.261±0.089	−0.007±0.001
10	−0.212±0.048	−0.845±0.121	−0.332±0.094	−0.011±0.008
15	−0.711±0.102	−1.016±0.289	−0.435±0.102	−2.760±0.985
20	−1.072±0.205	−1.311±0.314	−0.564±0.154	−3.558±0.786
25	−1.306±0.460	−2.001±0.467	−1.422±0.136	−3.464±0.765
30	−1.737±0.326	−2.006±0.465	−8.245±2.120	−3.328±0.639
[Ca^{2+}]=0.4 M				
5	−0.795±0.101	−0.178±0.022	−0.243±0.058	−0.012±0.010
10	−1.186±0.223	−0.206±0.037	−0.321±0.043	−0.054±0.002
15	−1.266±0.265	−0.256±0.032	−1.680±0.105	−2.604±0.704
20	−1.501±0.255	−0.562±0.045	−3.990±0.506	−3.805±0.806
25	−1.407±0.156	−1.260±0.102	−4.900±0.904	−4.240±0.458
30	−1.606±0.078	−2.126±0.098	−6.050±1.002	−4.512±0.512
[Mg^{2+}]=0.1 M				
5	−0.062±0.005	−0.180±0.045	−0.023±0.001	−0.026±0.001
10	−0.090±0.007	−0.344±0.079	−0.224±0.015	−0.038±0.003
15	−0.164±0.006	−0.820±0.092	−0.337±0.004	−0.106±0.021
20	−0.741±0.053	−0.826±0.099	−0.685±0.074	−0.247±0.045
25	−0.938±0.061	−0.998±0.099	−1.054±0.101	−0.452±0.037
30	−3.590±0.109	−7.760±1.107	−4.180±0.531	−3.131±0.705
[Mg^{2+}]=0.2 M				
5	−0.037±0.002	−0.234±0.023	−0.188±0.026	−0.101±0.018
10	−0.082±0.005	−0.384±0.042	−0.342±0.034	−0.092±0.012
15	−0.092±0.005	−0.416±0.042	−0.386±0.033	−0.428±0.036
20	−0.746±0.078	−0.518±0.033	−1.398±0.243	−0.974±0.080
25	−0.906±0.098	−0.648±0.026	−1.790±0.257	−1.214±0.099
30	−2.558±0.121	−2.056±0.254	−4.554±0.465	−1.992±0.101
[Mg^{2+}]=0.4 M				
5	−0.198±0.012	−0.534±0.074	−1.446±0.209	−0.322±0.015
10	−1.353±0.115	−1.796±0.209	−3.176±0.546	−1.525±0.309
15	−2.882±0.309	−4.276±0.587	−7.944±1.203	−1.697±0.452
20	−2.964±0.211	−5.732±0.725	−11.878±3.205	−1.866±0.505
25	−5.626±0.498	−7.188±0.899	−12.412±3.175	−1.914±0.311
30	−9.087±1.203	−7.664±0.911	−8.465±2.598	−3.701±0.928

monolayer augmented the effect is lower. A particular case was the X_{HDHC}=0.4 mixed system. Here at low Ca^{2+} subphase concentration (10 mM) the interactions are slightly favored (low negative $(\Delta G_{mix}{}^{E})$ and α values). As expected, α became positive with increasing [Ca^{2+}]. Nevertheless, a new increase of ion concentration leads to a diminution of the α parameter (rather than an increase) showing the existence of attractive interactions at the

monolayer. This fact was followed by a diminution of $(A_{1,2})_{\pi,}$, so it was supposed that part of molecules were removed from the interface.

The stabilizing effect of magnesium ion was less than the caused by Ca^{2+} presence, Fig. 8. This only can be appreciated at high π and $[Mg^{2+}]$=10 mM subphase concentration. As the amount Mg^{2+} augmented, all systems were stable at maximum compression, but the α absolute value decreased. A new increase of subphase Mg^{2+} concentration gave a noticeable disruption of monolayer and an alteration of intermolecular forces. The absolute α values augmented, indicating highly attractive or repulsive interaction. For X_{HDHC}=0.2, α= 22.5 at π=30 mJm^{-2} noticing very highly repulsive interactions. Similar behavior was seen for X_{HDHC}=0.8, while X_{HDHC}=0.4 and 0.6 were favored proportions (α= −12.5 and −20, respectively).

Conclusion

By joining the results of the preceding sections, a detailed picture of the characteristics of HDHC–DDAB mixed monolayers may be obtained. The behavior of such amphiphiles at the interface was clearly non-ideal and would be seriously influenced by the amount of Ca^{2+} or Mg^{2+} presence. Generally, the increment of subphase calcium content caused an augment of both pure and mixed systems limited area values, except for X_{HDHC}=0.2, 0.4, and 0.6 at $[Ca^{2+}]$=40 mM. On the other hand, when magnesium was present instead of calcium, almost all mixed monolayer showed $(A_{ex})\leq 0$ values, except for X_{HDHC}=0.4 at $[Mg^{2+}]$=10 mM and X_{HDHC}=0.4, 0.6 at $[Mg^{2+}]$=40 mM. These facts would be related to the different structure, thermodynamic affinity, and coordination properties of both cations. The monolayer stability was analyzed by the evaluation of thermodynamic parameters $(\Delta G_{mix}{}^{E})$ and α. Two effect could be noticed: (1) on one hand, the possibility of coordination bond formation between cations and carboxilate or carbonile groups in cholesteric ring and (2) on the other hand, the repulsive interactions with $R_2N^+(CH_3)_2$ groups. The delicate balance of both effect generated net repulsive or attractive forces at the interface. So, X_{HDHC}=0.6 and 0.8 at maximum surface compression (π=30 mJ m^{-2}, where it was determined that monolayers mimic bilayers) were always favored proportions at all calcium ion-tested concentrations. The X_{HDHC}=0.6 system was also stable in magnesium presence. The X_{HDHC}=0.2 mixed system go through a stable to an unstable state as the content of Ca^{2+} or Mg^{2+} augment. Finally, the X_{HDHC}=0.4 proportion presented a particular behavior. At low cation concentration, it was a favored proportion, unstable at intermediate concentration and stable again at high ion concentration. The effect was similar at Mg^{2+} presence. The information obtained is a first step towards the construction of smart materials.

Acknowledgements The authors acknowledge the financial support from the Universidad Nacional del Sur, Agencia Nacional de Promoción Científica y Tecnológica (ANPCyT), Concejo Nacional de Investigaciones Científicas y Técnicas de la República Argentina (CONICET), the Spanish "Ministerio de Educación y Ciencia" (Project MAT 2008-04722). JMR thank "Consellería de Educación e Ordenación Universitaria de Xunta de Galicia" and "Dirección Xeral de Promoción Científica e Tecnolóxica do Sistema Universitario de Galicia". PM is an adjunct researcher of (CONICET). MFL has a fellowship of the CONICET.

References

1. St-Pierre MV, Kullak-Ublick GA, Haganbuch B, Meier PJ (2001) Transport of bile acids in hepatic and non-hepatic tissues. J Exp Biol 204:1673–1686
2. Mukhopadhyay S, Maitra U (2004) Chemistry and biology of bile acids. Curr Sci 87(12):1666–1682
3. Ohtake S, Schebor C, Palecek SP, de Pablo JJ (2005) Phase behavior of freeze-dried phospholipid-cholesterol mixtures stabilized with trehalose. Biochim Biophys Acta (BBA)-Biomembr 1713(1):57–64
4. Hjelm RP Jr, Thiyagarajan P, Alkan-Onyuksel H (1992) Organization of phosphatidylcholine and bile salt in rodlike mixed micelles. J Phys Chem 96(21):8653–8661
5. Long AM, Kaler EW, Lee SP, Wingnall GD (1994) Characterization of lecithin-taurodeoxycholate mixed micelles using small-angle neutron scattering and static and dynamic light scattering. J Phys Chem 98(16):4402–4410
6. Jiang L, Wang K, Deng M, Wang Y, Huang J (2008) Bile salt-induced vesicle to micelle transition in catanionic surfactant systems: steric and electrostatic interactions. Langmuir 24:4600–4606, and references therein
7. Philp D, Stoddart JF (1996) Self-assembly in natural and unnatural systems. Angew Chem Int Ed 35:1154–1196
8. Tanford C (1980) The hydrophobic effect. Wiley, New York
9. Israelachvili JN (1992) Intermolecular and surface forces. Academic Press, London
10. Paul S, Patey GN (2007) The influence of urea and trimethylamine-*N*-oxide on hydrophobic interactions. J Phys Chem B 111(28):7932–7933
11. Messina PV, Ruso JM, Prieto G, Fernadez-Leyes M, Schulz P, Sarmiento F (2009) Thermodynamic and elastic fluctuation analysis of langmuir mixed monolayers composed by dehydrocholic acid (HDHC) and didodecyldimethylammonium bromide (DDAB). Colloids Surf B Biointerfaces 75:34–41
12. Gonzales YI, Nakanishi H, Stjerndahl M, Kaler EW (2005) Influence of pH on the micelle-to-vesicle transition in aqueous mixtures of sodium dodecyl benzenesulfonate with histidine. J Phys Chem B 109(23):11675–11682
13. Renoncourt A, Vlachy N, Bauduin P, Drechsler M, Touraud D, Verbavatz JM, Dubois M, Kunz W, Ninham BW (2007) Specific alkali cation effects in the transition from micelles to vesicles through salt addition. Langmuir 23(5):2376–2381
14. Ho SW, Jung D, Calhoun JR, Lear JD, Okon M, Scout WR, Hancock RE, Straus SK (2008) Effect of divalent cations on the structure of antibiotic daptomycin. Eur Biophys J 37(4):421–433

15. Akashi K, Miyata H, Itoh H, Kinosita K Jr (1998) Formulation of giant liposomes promoted by divalent catiions: critical role of electrostatic repulsion. Biophys J 74(6):2973–2982
16. Uhriková D, Kucerka N, Teixeira J, Gordeliy V, Balgavý P (2008) Structural changes in dipalmitoylphosphatidylcholine bilayer promoted by Ca2+ ions: a small-angle neutron scattering study. Chem Phys Lipids 155(2):80–89
17. Cabrerizo-Vilchez MA, Wege HA, Holgado-Terriza JA, Neumann AW (1999) Axisymmetric drop shape analysis as penetration Langmuir balance. Rev Sci Instrum 70(5):2438–2444
18. Wege HA, Holgado-Terriza JA, Cabrerizo-Vílchez MA (2002) Development of a constant surface pressure penetration langmuir balance based on axisymmetric drop shape analysis. J Colloid Interf Sci 249:263–273
19. Taylor JR (1982) An introduction to error analysis: the study of uncertainties in physical measurements. University Science Books, Sausalito-California. ISBN: 0935702075
20. Harkins WD (1954) The physical chemistry of surface films. Reinhold Publishing Co., New York, p 107
21. Gaines GL (1966) Insoluble monolayers at liquid gas interfaces. Wiley Interscience, New York
22. Adamson AW, Gast AP (1997) Physical chemistry of surfaces, 6th edn. Wiley, New York
23. Gau CS, Yu H, Zografi G (1994) Surface viscoelasticity of β-casein monolayers at the air/water interface by electrocapillary wave diffraction. J Colloid Interf Sci 162(1):214–221
24. Birdi KS (1989) Lipid and biopolymer monolayer at liquid interfaces. Plenun Press, New York
25. Tadros KDY, Deol B, Vollhardt H, Miller D, Cabrerizo-Vilchez MA R, Neumann AW (1996) Axisymmetric drop shape analysis as a film balance: rate dependence of the collapse pressure and molecular area at close packing of 1-octadecanol monolayers. Langmuir 12(7):1851–1859
26. Broniatowski M, Dynarowicz-Łątka P (2006) Semifluorinated chains at the air/water interface: studies of the interaction of a semi-fluorinated alkane with fluorinated alcohols in mixed langmuir monolayers. Langmuir 22(6):2691–2696
27. Rodríguez-Niño R, Carrera CS, Rodríguez-Patino JM (1999) Interfacial characteristics of β-casein spread films at the air–water interface. Colloids Surf B Biointerfaces 12(3–6):161–173
28. Peng JB, Barness GT, Gentle IR (2001) The structures of Langmuir–Blodgett films of fatty acids and their salts. Adv Colloid Interface Sci 91(2):163–219
29. Dynarowicz P, Romeo NV, Miñones Trillo J (1998) Stability of dialkyldimethylammonium bromides monolayers spread at the water/air interface. Colloid Surf A: Physicochem Eng Asp 131(1–3):249–256
30. Viseu MI, Gonçalves da Silva AM, Costa SMB (2001) Reorganization and desorption of catanionic monolayers. Kinetics of π–t and A–t relaxation. Langmuir 17(5):1529–1537
31. Hato M, Minamikawa H, Okamoto K (1993) Monolayers of ω-hydroxyalkyldimethyloctadecylammonium bromide at water-air interface. J Colloid Interface Sci 161(1):155–162
32. Fahey DA, Carey MC, Donovan JM (1995) Bile acid/phosphatidylcholine interactions in mixed monomolecular layers: differences in condensation effects but not interfacial orientation between hydrophobic and hydrophilic bile acid species. Biochemistry 34:10886–10897
33. Schulz P, Messina P, Morini M, Vuano B (2002) Potentiometric studies on sodium dehydrocholate micelles. Colloid Polym Sci 280:1104–1109
34. Vlachy N, Jagoda-Cwiklik B, Vácha R, Touraud D, Jungwirth P, Kunz W (2009) Hofmeister series and specific interactions of charged headgroups with aqueous ions. Adv Colloid Interface Sci 146:42–47
35. Zhang Y, Cremer PS (2006) Interactions between macromolecules and ions: the Hofmeister series. Curr Opin Chem Biol 10:658–663
36. Collins KD (2004) Ions from the Hofmeister series and omolytes: effects on proteins in solution and in the crystallization process. Methods 34:300–311
37. Alimenti G, Messina P, Morini MA, Schulz PC (2003) Evaporation studies on sodium dehydrocholate aqueous solution. Colloid Polym Sci 282:170–176
38. Sugihara G, Tanaka M (1978) Micelle formation of bile acids salts. Hyomen 16(9):537–554
39. Bock CW, Kaufman A, Glusker JP (1994) Coordination of water to magnesium cations. Inorg Chem 33(3):419–427
40. Chen KB, Chang CH, Yang YM, Maa JR (2000) On the interaction of dipalmitoyl phosphatidylcholine with normal long-chain alcohols in a mixed monolayer: a thermodynamic study. Colloids Surf A 170(2–3):199–208